Colloid Polym Sci (2004) 282: 502–510
DOI 10.1007/s00396-003-0974-2

ORIGINAL CONTRIBUTION

H. Sun
N. Venkatasubramanian
M.D. Houtz
J.E. Mark
S.C. Tan
F.E. Arnold
C.Y-C. Lee

Molecular composites by incorporation of a rod-like polymer into a functionalized high-performance polymer, and their conversion into microcellular foams

Received: 7 March 2003
Accepted: 17 July 2003
Published online: 5 September 2003

H. Sun · J.E. Mark (✉)
Department of Chemistry and the
Polymer Research Center,
The University of Cincinnati,
Cincinnati, OH 45221-0172, USA
E-mail: markje@email.uc.edu

N. Venkatasubramanian · M.D. Houtz
University of Dayton Research Institute,
300 College Park Drive, Dayton,
OH 45469, USA

S.C. Tan
1187 Richfield Center,
Wright Materials Research Co.,
Beavercreek, OH 45430, USA

F.E. Arnold
Polymer Branch, AFRL/MLBP,
Wright-Patterson Air Force Base,
Dayton, OH 45433-7750, USA

C.Y.-C. Lee
Directorate of Chemistry and Life Sciences,
AFOSR/NL, Arlington,
VA 22203-1977, USA

Abstract Molecular composites were prepared from sulfonated modifications of polysulfone and polyphenylsulfone by incorporating relatively stiff polybenzimidazole (PBI) chains into them. The composites were characterized by Fourier-transform infrared (FT-IR) spectroscopy, differential scanning calorimetry (DSC), thermal mechanical analysis (TMA), thermogravimetric analysis (TGA), and scanning electron microscopy (SEM). The FT-IR results demonstrated strong specific interactions between the sulfonated polymers and the PBI, which was presumed to be the reason for the enhanced miscibility observed. Miscibility was also indicated in the DSC and TMA results, by the presence of a single glass transition temperature (which was composition dependent), although there did appear to be a small degree of phase separation. TGA results showed improvements in the thermal stability of the polymer matrix because of the incorporation of PBI. Results from SEM were also consistent with considerable miscibility. Microcellular foams processed from these molecular composites had partial open-cell cell structures, with average cell sizes ranging from 0.2 to 5 μm, in unusual bimodal cell-size distributions.

Keywords Sulfonated polysulfone · Sulfonated polyphenylsulfone · Polybenzimidazole · Molecular composites · Microcellular foams

Introduction

Polymer-based composites have played a central role in materials science, and predominate in importance in structural applications. Relatively little has been done, however, to extend the science and technology developed for the bulk materials to composites in the form of foams (in spite of the obvious advantages such as reductions in weight). Foams without dispersed phases, in fact, already enjoy a very wide variety of applications. Most of these "conventional" foamed polymers, however, are limited to environments below approximately 200°C, and their mechanical properties degrade significantly at elevated temperatures [1]. Thus, conventional thermoplastic foams are not suitable at high temperatures, particularly in long-term applications. Alleviating this limitation is one of the aims of the present work. More generally, the goals are the preparation, characterization, and evaluation of polymer-based foams of sufficient toughness and high-temperature resistance to

be used as structural materials in US Air Force applications. One example is the need for foams with higher softening temperatures and increased thermal stabilities for use in wing structures that now experience increasing temperatures as flight speeds increase. In studies [2, 3, 4] in this series thus far, the focus has been on commercially available high-performance thermoplastics, including a polysulfone, a polyethersulfone, a polyphenylsulfone, a polyetherimide, and a poly(ether ketone ketone). These polymers were successfully processed into microcellular foams using the two-step batch foaming process developed by Suh et al. [5, 6, 7] and the processing parameters thus established lay the groundwork for both the present investigation and future studies.

In order to further enhance the thermal stabilities and the mechanical properties of these microcellular foams, a rod-like polymer, polybenzimidazole (PBI) of superior thermal and mechanical properties [8] was blended into the host polymer matrices. These stiff polymer chains can increase the toughness and the thermal resistance of the thermoplastic phase, particularly when strong interfacial bonding can be designed into the structures. In some cases, the rod polymer is dispersed almost to the molecular level, resulting in what have been called "molecular composites" [9, 10, 11, 12]. At these nanoscale levels, partial miscibility makes it difficult to distinguish between composites and the usual molecular dispersions called solutions.

Since Suh and his colleagues patented the microcellular foaming technique in 1984 [5], there has been an increasing interest in this area. This foaming technique has been successfully applied to a variety of polymers [13, 14, 15], including amorphous, partially crystalline thermoplastics, some thermosets, liquid-crystalline polymers, and even elastomers. Less has been done with composites [16, 17, 18, 19] in general, and almost nothing on the molecular composites [20] addressed in the present investigation In this case, having rigid chains aligned along the foam struts or within the foam walls should be particularly effective with regard to improving mechanical properties. Such foamed molecular composites should have superior thermal and mechanical properties, making them high-performance materials. In particular, their being lightweight and good insulators suggests potential applications in a variety of fields, including the military.

In the present study, sulfonated polysulfone (S-PSF) and polyphenylsulfone (S-PPSF) with sulfonation degree of approximately 0.5 were employed as the sodium salts S-PSF(Na) and S-PPSF(Na). Samples of these two matrix polymers were blended with various amounts of PBI in solution, and films were obtained by solution casting. The resulting S-PSF(Na)/PBI and S-PPSF(Na)/PBI composite films were characterized by Fourier-transform infrared (FT-IR) spectroscopy, differential scanning calorimetry (DSC), thermal mechanical analysis (TMA), thermogravimetric analysis (TGA), and scanning electron microscopy (SEM). Microcellular foams were also processed from these composite films.

Experimental

Materials

Samples of a polysulfone (PSF, Udel P-1700) and a polyphenylsulfone (PPSF, Radel R-5000) were kindly supplied by the BP-Amoco Corporation, Marietta, Ohio, USA. Values of their glass transition temperature T_g and density ρ_m were, PSF: 185°C and 1.34 g/cm^3, and PPSF: 220°C and 1.29 g/cm^3. A sample of PBI powder with a mean particle size of 100 μm was purchased from Goodfellow Corporation, Huntingdon, UK. All polymer samples were dried overnight at approximately 130°C before use. Dimethylsulfoxide (DMSO), N,N-dimethylacetamide (DMAC) and N,N-dimethylformamide (DMF) were obtained from the Aldrich Company, Milwaukee, Wis., USA and used as received. All other chemicals were purchased from Aldrich, and were employed as described in the literature for sulfonation of PSF and PPSF [21, 22]. Carbon dioxide (99.9%) was obtained from Wright Brothers Inc., Cincinnati, Ohio, USA.

Sulfonation of polysulfone and polyphenylsulfone

Sulfonated polysulfone was prepared as described by Johnson [21], with slight modification [23], using SO_3/triethylphosphate (TEP) (2:1 molar ratio) complex as the sulfonation agent. This agent was prepared as follows: 4.0 ml TEP was mixed with 40 ml dichloroethane in an ice bath under argon. Then, 3.8 g of SO_3 was added quickly to this mixture, which was stirred in an ice bath until all the SO_3 dissolved and the solution turned yellow (indicating the formation of the desired complex). This sulfonation agent was added slowly to 20 g of the PSF dissolved in 200 ml of dichloroethane using a syringe under argon with vigorous stirring at room temperature. The resulting sulfonated polysulfone precipitated in its acid form and the resulting slurry was stirred for another 2 h. The slurry was poured into a large amount of isopropanol and the precipitated material was filtered, washed twice in dichloroethane, and then dried under vacuum at 50°C for about 24 h. The yield was approximately 92% and the degree of sulfonation was 0.5. The sodium salt form S-PSF(Na) was prepared by neutralization of the S-PSF acid with a sodium methoxide/water solution as follows: 15 g of the S-PSF acid form was dissolved in 150 ml DMF, 5 g sodium methoxide dissolved in distilled water was slowly added to this solution, and the solution was stirred at room temperature overnight. A white solid was obtained by precipitation of the resulting slurry into isopropanol. It was washed several times in warm water for 4–6 h to remove the inorganic salt trapped in the polymer, and was then dried at 100°C under vacuum. In the sulfonated polyphenylsulfone case, dichloromethane was used as solvent instead of dichloroethane; all other procedures were the same. The yield was about 95%.

Preparation of the S-PSF(Na)/PBI and S-PPSF(Na)/PBI composites

PBI was only partially soluble in DMAC or DMF at normal pressures, but the mixed solvent DMAC/DMSO or DMF/DMSO at a 1:1 volume ratio was found to dissolve it completely at atmospheric pressure. This permitted preparation of a 2% PBI

solution (w/v) by mixing 2 g of dried PBI into 100 ml of the DMSO/DMAC or DMSO/DMF solvent mxture. This was followed by heating at the reflux temperature (approximately 175°C) for 2 h, to ensure dissolution. This gave a clear orange solution that could be used for the formation of composite films. Varying amounts of the S-PSF(Na) or S-PPSF(Na) were dissolved in this 2% PBI solution. The concentrations of the solutions were kept in the range 7–10% (w/v). The mixtures were stirred at 70°C for about 8 h, the clear solutions were poured into Petri dishes, and the solvent evaporated at 100°C. Transparent yellow-to-orange films (about 0.2–0.5 mm in thickness) were obtained and vacuum dried at 100°C for about 24 h, and were then heated to 200°C and further dried for approximately 24 h to remove as much of the residual solvent as possible.

Preparation of microcellular foams

Microcellular foams were prepared from these composite films using the two-step batch process as described elsewhere [2, 3]. Briefly, the films were saturated in a pressure vessel with CO_2 gas maintained at 800 psi at room temperature. Upon saturation, the samples were removed from the pressure vessel and foamed in an oil bath maintained at the desired temperature.

Characterization of the S-PSF(Na)/PBI and S-PPSF(Na)/PBI composite films

Very thin films (about 0.05 mm thick) were prepared for FT-IR analysis. The spectra of the composite films were recorded on a Bruker IFS 28 FT-IR spectrometer (Bruker Optics Inc., Billerica, MA, USA), using 30 scans for each analysis. For the SEM tests, both the composite film and the corresponing microcellular foam samples were frozen in liquid nitrogen and fractured to ensure that the microstructure remains clean and intact. The fractured surfaces were coated with gold using a sputter coater, and photographed with a Hitachi S-4000 SEM (Hitachi Instrument Inc., CA, USA). DSC was carried out using a DSC-2910 apparatus. In the first scan, the samples were heated to 260°C in nitrogen and quenched, and then the second scan was recorded. The middle points of the heat capacity change were taken as the glass transition temperature (T_g). TGA experiments were performed with a 2950 TGA unit in air with a heating rate of 10°C/min. TMA tests were carried out with TMA-2940 equipment. The tests were done in film/fiber mode at 4°C/min heating rate with a 50 ml/min dry nitrogen flow. All the equipment for thermal analysis was from TA Instruments (New Castle, DE, USA).

Results and discussion

Characterization of the S-PSF(Na) and S-PPSF(Na)

The 2:1 SO_3/TEP complex was found to be a very effective sulfonation agent for the polysulfones. The reaction occurred very rapidly at room temperature and the sulfonation degree could easily be controlled by varying the ratio of SO_3/TEP to PSF or PPSF. There was no obvious degradation or cross-linking occurring during the sulfonation, judging from the fact that the reduced viscosities of the solutions remained essentially constant [22, 24]. Although of primary interest in the present investigation was the use of sulfonated polysulfone in molecular composites, it has been widely studied in membrane applications [25, 26, 27, 28, 29, 32], for example, for reverse osmosis [25, 26], ultrafiltration [27, 28], asymmetric devices [29, 30], and fuel cells [31, 32]. The sulfonated polyphenylsulfone, on the other hand, has not been investigated much at all [33]. In this paper, we present results on S-PSF(Na), S-PPSF(Na), and their composites.

The FT-IR spectrum for the S-PPSF(Na) is shown in Fig. 1. The characteristic peak caused by the symmetric stretching vibration of the sulfonate group (1,025 cm^{-1}) [21, 22] was clearly shown in the IR for the S-PPSF(Na). This result suggested that the sulfonate groups were successfully introduced into the polymer chains. In addition, the sulfonation degree of S-PPSF could also be readily controlled by varying the ratio of SO_3/TEP to PPSF. It was clear that the intensity of the sulfonate group peak increased as the sulfonation degree increased. The results thus support the desired chemical modifications, as summarized by the structures listed in Table 1.

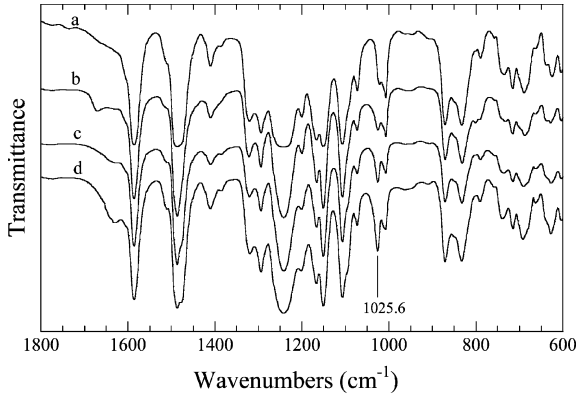

Fig. 1 FT-IR spectra for S-PPSF(Na) having various degrees of sulfonation: **a** 0.2, **b** 0.5, **c** 0.7, and **d** 1.0

Table 1 Chemical structures of the relevant polymers

Polymer	Structure
S-PSF(Na)	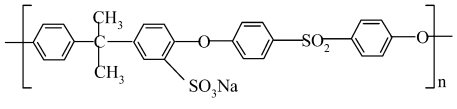
S-PPSF(Na)	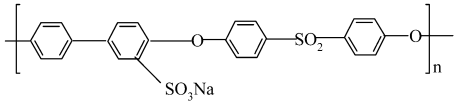
PBI	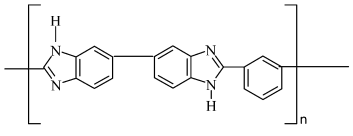

Characterization of the S-PSF(Na)/PBI and S-PPSF(Na)/PBI molecular composites

Improved miscibility

PBI itself exhibits high thermal stability and a very high T_g of approximately 410°C, which has encouraged its use as the dispersed phase in some high-T_g polymer blends [34, 35, 36]. With regard to such matrix polymers, PSF and PPSF are known to be immiscible with PBI and to form relatively unattractive incompatible systems [37, 38]. In fact, blending this rod-like polymer into any thermoplastic matrix generally results in phase separation. This immiscibility problem may be ameliorated, however, by inducing strong favorable interactions between the two polymers through the introduction of functional groups such as sulfonate into some of the chains [9, 10, 11, 12, 39, 40, 41, 42, 43]. Such interactions could be of the type ion–ion, ion–dipole, or acid–base. Most relevant here are reports [44, 45] that sulfonated polysulfone (S-PSF) can form such miscible blends with PBI, with documentation of the effects of degree of sulfonation and the ratio of PBI to S-PSF.

Early experiments in which S-PSF and S-PPSF in acid form were mixed into PBI solutions, gave immediate precipitations. These yellow precipitated phases could be neither dissolved in any ordinary solvent nor melt processed even at very high temperatures (350°C). The precipitant was probably the salt formed by S-PSF and S-PPSF acid with PBI, which is a base. In strong contrast, the sulfonate salts of PSF and PPSF dramatically increased their miscibility with PBI and resulted in miscible blends at least at some compositions and degrees of sulfonation. The results of characterizing these yellow-to-orange transparent films with FT-IR, DSC, TMA, TGA and SEM are presented below.

FT-IR analysis

The IR spectra of the S-PSF(Na)/PBI materials with high PBI contents have been thoroughly examined by Deimede et al. [44]. In the present study, however, we examined the IR spectra of the S-PPSF(Na)/PBI composites at relatively low PBI contents. The FT-IR spectra of the polymer and the composites are presented in Fig. 2. For pure PBI four peaks were clearly shown in the N–H stretching region (2,800–3,500 cm^{-1}), consistent with the literature [44]: the peak at 3,403 cm^{-1} was attributed to non-hydrogen bonded or "free" N–H groups, those at 3,143 and 3,194 cm^{-1} were assigned to self-associated hydrogen bonded N–H groups, and that at 3,063 cm^{-1} was attributed to the stretching vibration of aromatic C–H groups. Upon blending the PBI with S-PSF(Na) or S-PPSF(Na), the self-associated hydrogen bonded N–H peaks shifted to higher wavenumbers,

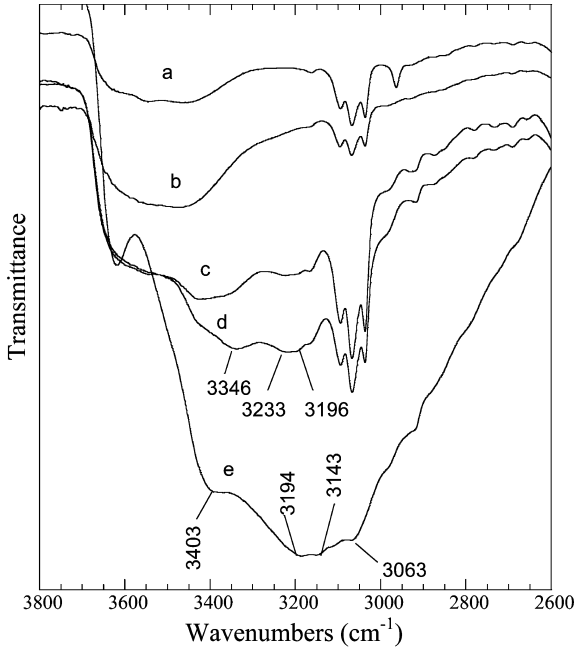

Fig. 2a–e FT-IR spectra for S-PPSF(Na)/PBI molecular composites. Parts **a**–**e** correspond to the compositions: **a** S-PPSF(Na), **b** 90/10, **c** 80/20, **d** 70/30, and **e** pure PBI

3,196 and 3,233 cm^{-1} for S-PPSF(Na)/PBI (at 80/20 and 70/30 (w/w) compositions). This frequency shift suggested weakening of the self-associated N–H—N hydrogen bonding. The "free" N–H peak in PBI shifted from 3,403 to 3,346 cm^{-1}; these spectral changes presumably arise because of the ion–dipole as well as hydrogen bonding interactions between the sodium sulfonate pendants in S-PSF(Na) or S-PPSF(Na) and the imidazole ring of PBI. The 1,028 cm^{-1} band, which is characteristic of the sulfonate group, also exhibits a slight decrease in stretching frequency with increase in PBI content (not shown here). From the results of this IR examination, there is clear evidence for specific interaction between S-PSF(Na) or S-PPSF(Na) and PBI, resulting in enhanced blend miscibility.

Differential scanning calorimetry (DSC) analysis

Figure 3 represents the DSC curves of S-PSF(Na), S-PPSF(Na) and their composites with PBI. The T_g, s for pure PSF and PPSF are 184 and 218°C, respectively. With the introduction of SO_3Na groups at a degree of 0.5, S-PSF(Na) showed a higher T_g (233°C, in Fig. 3a) and S-PPSF(Na) at 250°C (Fig. 3b). This is consistent with results of Johnson [21] and Noshay [22] for S-PSF(Na), although the value of T_g was slightly lower than their results. The introduction of SO_3Na pendant groups into the polysulfone backbone increases its T_g,

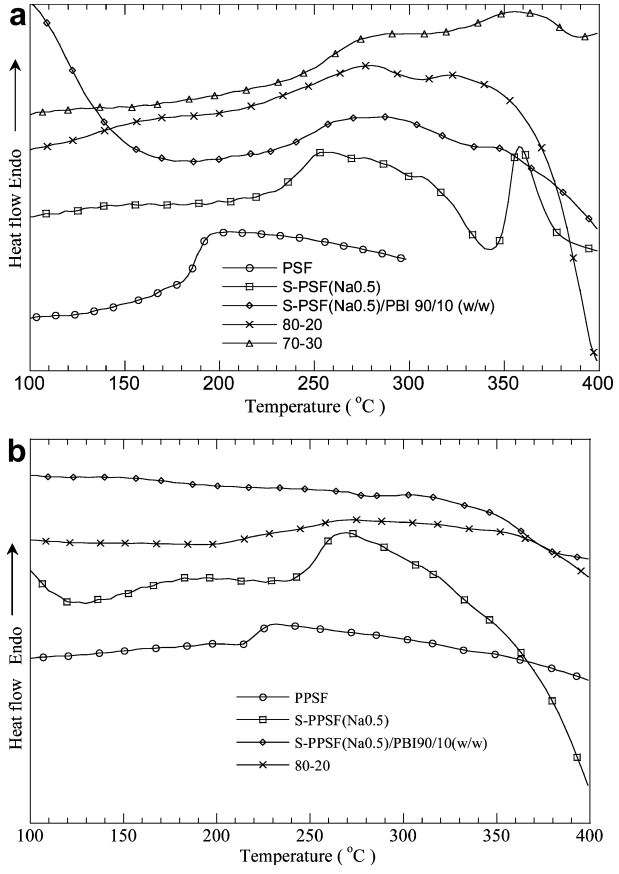

Fig. 3 DSC curves for **a** S-PSF(Na)/PBI, and **b** S-PPSF(Na)/PBI composites

ascribable to increased intermolecular associations through the pendant $SO_3^-Na^+$ functionality, thus restricting the mobility of the chain segments. An endothermic peak at around 360°C was observed for S-PSF(Na). This could be due to first-stage decomposition of S-PSF(Na) at this temperature (will be described in TGA analysis).

With the addition of PBI, DSC shows a single but relatively broad glass transition for all the S-PSF(Na)/PBI compositions, also, as shown in Fig. 3a, increase in PBI content was found to monotonically increase the T_g of the S-PSF(Na)/PBI composites. This observation indicates significant compatibility of the blend components. Careful examination of the DSC curves of S-PSF(Na)/PBI composites revealed that in addition to these glass transitions, there was another weak transition in the temperature range 320–360°C, somewhat apparent for the 80/20 and 70/30 compositions. This may be tentatively attributed to partial phase separation at higher temperatures, occurring in S-PSF composites with higher PBI content, causing some segregation of PBI-rich domains or the first-stage decomposition. For the S-PPSF(Na)/ PBI composites, no distinctive T_g could be observed by DSC.

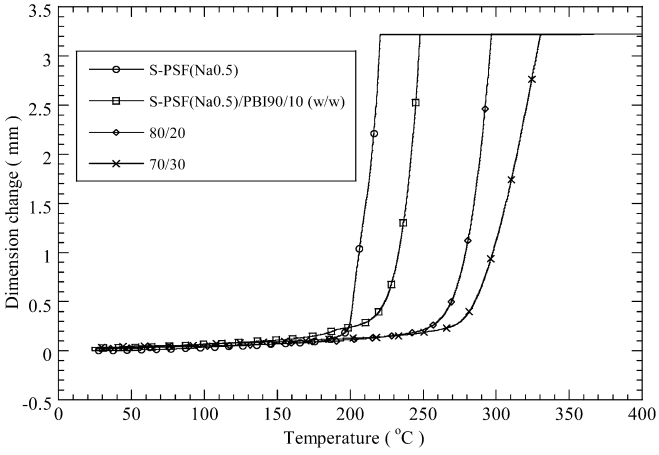

Fig. 4 TMA traces for the S-PSF(Na)/PBI molecular composites

Table 2 Values of the glass transition temperature T_g of the S-PSF(Na)/PBI composites as determined by DSC, TMA and predicated by theory

Composition (w/w)	DSC (°C)	TMA (°C)	Fox equation (°C)
100/0	235.0	198.5	235.0
90/10	242.4	232.5	243.5
80/20	258.3	266.0	255.0
70/30	265.1	280.2	267.0
0/100	409.8	–	409.8

Thermal mechanical analysis (TMA)

TMA traces for the S-PSF(Na)/PBI composites are depicted in Fig. 4. They show the same trend as the DSC results, specifically the occurrence of a single T_g, with values increasing with increase in PBI content, although the T_g values are somewhat different from those obtained by DSC. (They were lower for S-PSF(Na) and the S-PSF(Na)/PBI 90/10 composition, but higher for the 80/20 and 70/30 compositions.) Table 2 provides a comparison of the experimental values of T_g from DSC and TMA with theoretical values calculated from the Fox equation [46]. The comparison shows that the DSC values match very well with those from theory.

Fox equation:

$$\frac{1}{T_g} = \frac{w_1}{T_{g1}} + \frac{w_2}{T_{g2}} \tag{1}$$

where w_i is the weight fraction and T_{gi} is the glass transition temperature of component i.

For the S-PPSF(Na, sulfonation degree of 0.5)/PBI composites, TMA, however, did show clear transitions, although the values of T_g were lower than expected, as is shown by the dimensional changes in Fig. 5a. The T_g was around 210°C for 90/10 (w/w) composition. For the 80/20 and 70/30 compositions, however, small dimen-

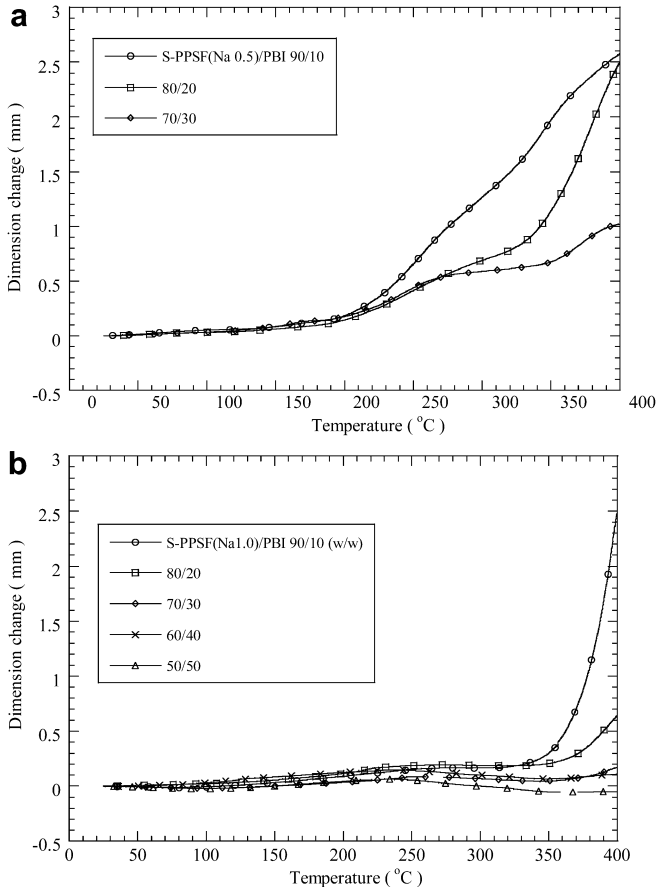

Fig. 5 TMA traces for the S-PPSF(Na)/PBI composites at various degrees of sulfonation: **a** 0.5, and **b** 1.0

sional changes were also observed from 190 to 250°C. The dimensions changed more markedly with temperature above 335°C for the 80/20 samples, and above 350°C for the 70/30 samples. One plausible explanation takes into account the presence of traces of the relatively less volatile residual solvents DMAC and DMSO. The dimensional changes in the 190–250°C range in the TMA experiments could be either caused by the volatilization of these residual solvents or by the plasticizing effect on the polymer blends, thus lowering their values of T_g.

The sulfonation degree of S-PPSF(Na, sulfonation degree of 1) was also found to affect the T_g, s of the S-PPSF/PBI composites, as shown in Fig. 5b. Only a single T_g, indicative of miscibility between the two polymer components, was observed for each composition; the T_g, s had dramatically increased, to 340, 365, and 380°C for the 90/10, 80/20, and 70/30 compositions, respectively. For higher PBI contents, 60/40 and 50/50, there was no obvious dimensional change even at 400°C. These high values of T_g made it very difficult to process these composites, and our attempts to fabricate foams from these composites were not successful.

Thermogravimetric analysis (TGA)

The thermal stabilities of the composites were measured by TGA in air. The TGA traces of composites at 80–100% weight range are presented in Fig. 6. The occurrence of PBI decomposition begins around 530°C. For the S-PSF(Na) and S-PPSF(Na), the TGA traces show a two-stage decomposition profile. The first-stage decomposition spanned from 240 to 380°C, causing an approximate 4–6% weight loss owing to loss of SO_2 and SO_3 from the sulfonated groups. The first degradation temperature is much higher than that of S-PSF in acidic form since the sulfonate salt pendants are much more thermally stable than the sulfonic acids. After the first stage, the polymers decomposed quickly with temperature until at 500°C for S-PSF(Na) and 590°C for S-PPSF(Na) catastrophic degradation occurred. With the addition of PBI to form composites, the first-stage decomposition gradually became less obvious and shifted to a higher temperature range, 290–390°C for S-PSF(Na)/PBI and 320–430°C for S-PPSF(Na)/PBI. After that the composites were found to degrade more gradually with the temperature. At 500°C, they showed weight losses of less than 25 wt%. When the temperature was increased to 530°C (at which PBI begins to decompose), there was still considerable weight remaining, around 60–75%, depending on the PBI content. For the S-PSF(Na)/PBI composites, the final decomposition temperatures were approximately 550, 580, and 600°C at 90/10, 80/20, and 70/30 compositions, respectively. For the S-PPSF(Na)/PBI composites, the decomposition profiles showed a similar trend but were found shifted to even higher temperatures, as is shown in Fig. 6b. This was, in part, due to the fact that the second-stage decomposition of S-PPSF(Na) occurred at a significantly higher temperature than that for S-PSF(Na).

Morphologies of the molecular composites

The composites obtained from PBI and S-PSF(Na), S-PPSF(Na) were optically clear, yellow-to-orange films that appeared homogeneous; this transparency suggested miscibility on a scale down to 100 nm. Some typical SEM micrographs of the fractured surface are presented in Fig. 7. At low PBI contents (Figs. 7a and b), the fracture surface is essentially featureless, and there are no distinct domains or domain boundaries on the scale probed by SEM (ca. 20 nm). An essentially co-continuous microstructure [47] was observed, which is an indication of good miscibility. The sparse dots (about 20–40 nm), seen to be randomly distributed in the micrographs suggest a small degree of phase separation, possibly occurring during the evaporation of solvent, but at high PBI contents (Figs. 7d and c), the

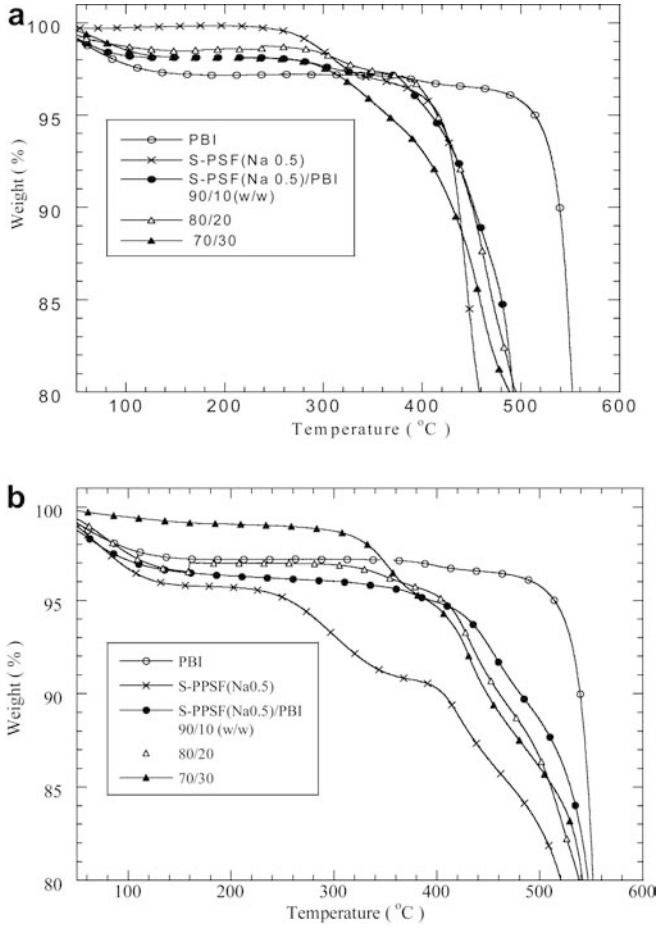

Fig. 6 TGA traces for **a** S-PSF(Na)/PBI, and **b** S-PPSF(Na)/PBI composites

morphology of the as-cast composites was significantly different from that observed for the blends with low PBI contents. It shows the presence of very uniform spherical particles, about 30–50 nm in size, of the dispersed phase, which could be either PBI or S-PSF(Na).

These composites did show the thermally induced phase separation as reported by Chuah et al. for poly (*p*-phenylenebenzobisthiazole)/nylon 66 molecular composites [48]. Specifically, after heating to 280°C for 0.5 h, distinct phase separation did appear in the micrographs, as shown in Fig. 8. At such temperatures, which are much higher than the values of T_g for S-PSF(Na), the polymer chains have considerable mobility and the increased segmental motions could have contributed to the microphase separation. The resulting domain size of 20–60 nm is considerably less than 100 nm, so the films remained optically clear.

Microcellular foams from the molecular composites

These composites were also processed into microcellular foams. In these cases, variables in addition to foaming temperature and foaming time were found to be important, including (i) composition of the blend, (ii) extent of phase separation in the composite, (iii) amount of any residual solvent present, (iv) thickness of the sample, and (v) CO_2 content upon saturation. As a result, the foaming behavior and morphologies of the resulting composite foams were much more complicated than those of the pure polymers. In general, the initial foaming temperature had to be higher for the composites. For example, the initial foaming temperature was

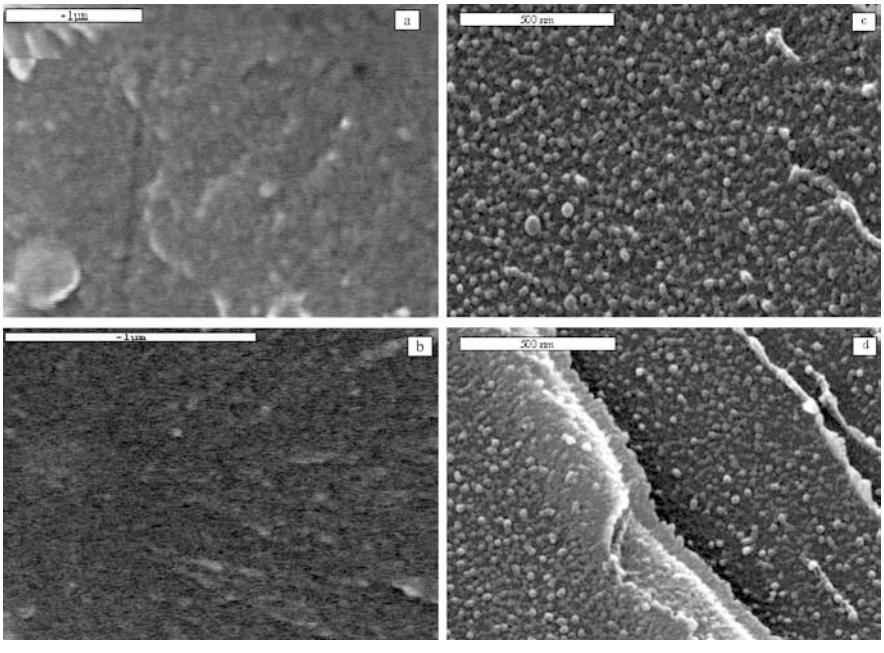

Fig. 7 SEM micrographs for **a** S-PSF(Na)/PBI 90/10, **b** S-PPSF(Na)/PBI 90/10, **c** S-PSF(Na)/PBI 50/50, and **d** 33.3/66.7

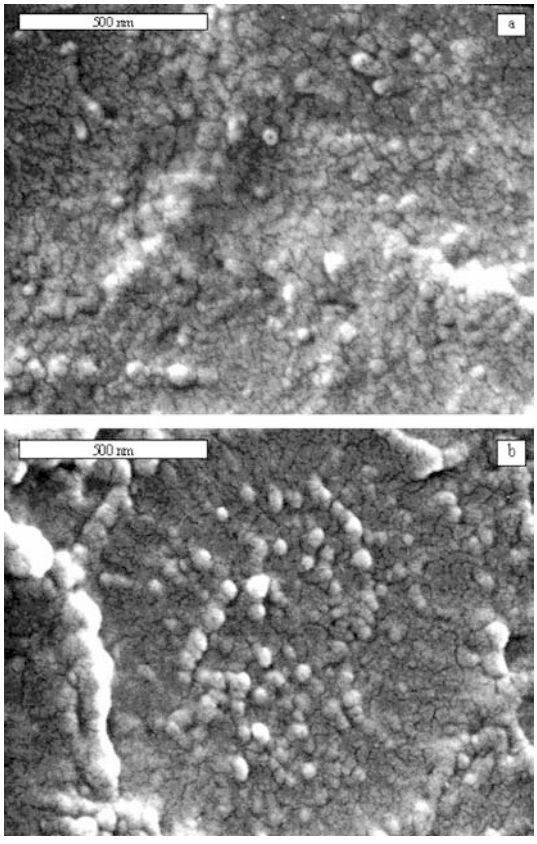

Fig. 8 SEM micrographs of **a** S-PSF(Na)/PBI (90/10), and **b** S-PPSF(Na)/PBI (90/10) after heating to 280°C for 0.5 h

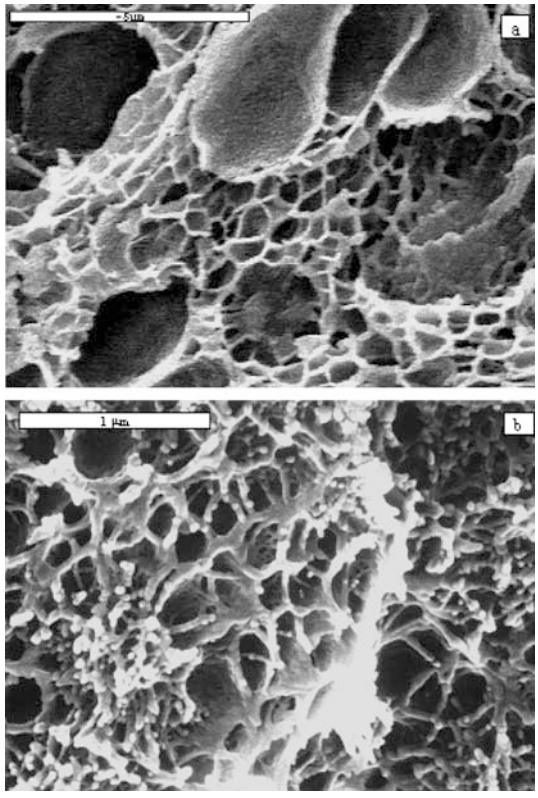

Fig. 9 Some typical SEM micrographs of microcellular foams prepared from: **a** S-PSF(Na)/PBI 90/10 foamed at 230°C, **b** S-PPSF(Na)/PBI 90/10 respectively, foamed at 185°C

100 and 120°C respectively for PSF and PPSF, but for the S-PSF(Na)/PBI composite at 90/10 composition, this temperature had to be increased to around 160°C, and the 80/20 composition gave only partially foamed structures at this temperature. Similar results had been reported by Krause et al. [20] for polysulfone/polyimide (Matrimid) composites, with the temperatures required increasing with increasing Matrimid content.

The morphologies of the composite foams are also significantly different from those of the PSF and PPSF foams. The PSF and PPSF foams have well-defined, closed-cell, spherical or polyhedral cell structures [2, 3]. The composite foams have unusual bimodal and partially open-cell structures, which were dependent on the foaming temperature, composition, residual solvent, and CO_2 content. Two typical SEM micrographs of microcellular foams prepared from composites are shown in Fig. 9. The bimodal structure may have been caused by microphase separation that occurred during the foaming process. The open-cell structures are probably caused by the residual solvent during the expansion of the polymer, resulting in the interconnected cells. This is consistent with Krause et al. [49, 50] reporting open-cell structures for microporous materials prepared from polysulfone and polysulfone/polyimide composites when there was a trace of solvent as a ''pore opener''. Additional results on these composite foams will be reported separately in the near future. Efforts are underway to extend some of these studies to the preparation of bulk samples that would be suitable for mechanical testing.

Conclusion

Introduction of sulfonate groups into PSF and PPSF can greatly increase their miscibility with PBI, because of the strong intermolecular interactions between the two components. The miscibility is indicated by the appearance of a single, composition-dependent T_g for the composites in DSC and TMA. The significant increase in T_g as well as in thermal stability demonstrated a well-defined synergistic effect. High-performance molecular composites were thus successfully prepared by the incorporation of rod-like PBI molecules into sulfonated polysulfone matrices. Microcellular foams were successfully prepared from high-performance molecular

composites. These novel microcellular foams with the partial open-cell structures might have some applications as high-performance structural materials or as membranes.

Acknowledgements It is a pleasure to acknowledge the financial support provided by the Air Force Office of Scientific Research (Directorate of Chemistry and Materials Science) through grant F49620-98-1-0319.

References

1. Hardy EF, Saunders JH (1972) In: Frisch KC, Saunders JH (eds) Plastics foams, vol 2. Marcel Dekker, New York, p 735
2. Sun H, Mark JE (2002) J Appl Polym Sci 86:1692
3. Sun H, Sur GS, Mark JE (2002) Eur Polym J 38:2373
4. Tan SC, Bai Z, Sun H, Mark JE, Arnold FE, Lee CYC (2003) J Mater Sci (in press)
5. Martini JE, Waldman FA, Suh NP (1984) US Patent 4,473,665
6. Martini JE, Waldman FA, Suh NP (1982) SPE Tech Paper 1:674
7. Kumar V, Suh NP (1990) Polym Eng Sci 30:1323
8. Buckley A, Stuetz DE, Seard GA (1985) In: Mark HF, Bikales NM, Overberger CG, Menges G (eds) Encyclopedia of polymer science and engineering, vol 11. Wiley, New York, p 572
9. Schartel B, Wendorff JH (1999) Polym Eng Sci 39:128
10. Arnold Jr FE, Arnold FE (1994) Adv Polym Sci 117:258
11. Pawlikowski GT, Dutte D, Weiss RA (1991) Ann Rev Mater Sci 21:159
12. Helminiak TE, Benner CL, Husman GE, Arnold FE (1980) US Patent 4,207,407
13. Baldwin DF, Tate D, Park CB, Cha SW, Suh NP (1994) J Jpn Soc Polym Proc (Seikei-kakou) 6:187
14. Baldwin DF, Tate D, Park CB, Cha SW, Suh NP (1994) J Jpn Soc Polym Proc (Seikei-kakou) 6:246
15. Park CB, Suh NP (1996) Polym Eng Sci 36:34
16. Nam PH, Maiti P, Okamoto M, Kotaka T, Nakayama T, Takada M, Ohshima M (2002) Polym Eng Sci 42:1907
17. Okamoto M, Nam PH, Maiti P, Kotaka T, Nakayama T, Takada M, Ohshima M, Usuki A, Hasegawa N, Okamoto H (2001) Nano Lett 1:503
18. Matuana LM, Park CB, Balatinecz JJ (1997) Polym Eng Sci 37:1137
19. Matuana LM, Park CB, Balatinecz JJ (1998) Polym Eng Sci 38:1862
20. Krause B, Diekmann K, van der Vegt NFA, Wessling M (2002) Macromolecules 35:1738
21. Johnson BC, Yilgor I, Tran C, Iqbal M, Wightman JP, Lloyd DR, McGrath JE (1984) J Polym Sci Polym Chem Ed 22:721
22. Noshay A, Robeson LM (1976) J Appl Polym Sci 20:1885
23. Sun H (2003) PhD thesis, University of Cincinnati
24. Byun IS, Kim CI, Seo JW (2000) J Appl Polym Sci 76:787
25. Yang MH (1995) Polym Testing 14:415
26. Vanzyl AJ, Kerres JA, Cui W, Junginger M (1997) J Membr Sci 137:173
27. Malaisamy R, Mehendran R, Mohan D, Rajendran M, Mohan V (2002) J Appl Polym Sci 86:1749
28. Malaisamy R, Mehendran R, Mohan D J (2002) J Appl Polym Sci 84:430
29. Kdela V, Richau K, Bleha M, Paul D (2001) Separat Purific Technol 22:655
30. Blanco JF, Nguyen, QT, Schaetzel P (2002) J Appl Polym Sci 84:2461
31. Manea C, Mulder M (2002) J Membr Sci 206:443
32. Manea C, Mulder M (2002) Desalination 147:179
33. Dyck A, Fritsch D, Nunes SP (2002) J Appl Polym Sci 86:2820
34. Xu ZL, Chung TS, Loh KC, Lim BC (1999) J Membr Sci 158:41
35. Foldes E, Fekete E, Karasz FE, Pukanszky B (2000) Polymer 41:975
36. Chung TS, Xu ZL (1998) J Membr Sci 147:35
37. Chung TS, Click M, Power EJ (1993) Polym Eng Sci 33:1042
38. Chung TS (1993) Polym Eng Sci 34:428
39. Parker G, Hara M (1997) Polymer 38:2701
40. Hara M, Parker GJ (1992) Polymer 33:4650
41. Tan LS, Arnold FE, Chuah HH (1991) Polymer 32:370
42. MacKnight WJ, Sakurai K, Douglas EP (1992) Macromolecules 25:4506
43. Gieselman MB, Reynolds JR (1990) Macromolecules 23:3118
44. Deimede V, Voyiatzis GA, Kallitsis JK, Qingfeng L, Bjerrum NJ (2000) Macromolecules 33:7609
45. Hasiotis C, Deimede V, Kontoyannis C (2001) Electrochim Acta 46:2401
46. Strobl G (1997) The physics of polymers, 2nd edn. Springer-Verlag, Berlin Heidelberg New York
47. Venkatasubramanian N, Dean DR, Dang TD, Price GE, Arnold FE (2000) Polymer 41:3213
48. Chuah HH, Kyu T, Helminiak TE (1987) Polymer 28:2130
49. Krause B, Sijbesma HJP, Munuklu P, van der Vegt NFA, Wessling M (2001) Macromolecules 34:8792
50. Krause B, Boreeigter ME, van der Vegt NFA, Strathmann H, Wessling M (2001) J Membr Sci 187:181